Available online at www.sciencedirect.com
SCIENCE DIRECT®
Talanta 65 (2005) 1126–1131
Talanta
www.elsevier.com/locate/talanta

Voltammetric and waveguide spectroelectrochemical characterization of ultrathin poly(aniline)/poly(acrylic acid) films self-assembled on indium-tin oxide

Chenhao Ge, Walter J. Doherty III, Sergio B. Mendes, Neal R. Armstrong, S. Scott Saavedra*

Department of Chemistry, University of Arizona, Tucson, AZ 85721-0041, USA

Received 23 February 2004; received in revised form 14 July 2004; accepted 27 July 2004
Available online 25 November 2004

Abstract

We report on the spectroelectrochemical characterization of conducting polymer (CP) films, composed of alternating layers of poly(aniline) (PANI) and poly(acrylic acid) (PAA), deposited on ITO-coated, planar glass substrates using layer-by-layer self-assembly. Absorbance changes associated with voltammetrically induced redox changes in ultrathin films composed of only two bilayers (ITO/PANI/PAA/PANI/PAA) were monitored in real time using a unique multiple reflection, broadband attenuated total reflection (ATR) spectrometer. CP films in contact with pH 7 buffer undergo a single oxidation/reduction process, with ca. 12.5% of the aniline centers in the film being oxidized and reduced. The ATR spectra indicate that during an anodic sweep, the leucoemeraldine form of PANI in these films is oxidized to generate both the emeraldine and pernigraniline forms simultaneously. A comparison of the behavior observed during anodic and cathodic sweeps suggests that the rate of oxidation is limited by structural changes in the polymer film originating in electrostatic repulsion between positively charged PANI chains.

Keywords: Spectroelectrochemistry; Conducting polymer; Poly(aniline); ATR spectroscopy

1. Introduction

The optical and electronic properties of poly(aniline) (PANI) films supported on electrode surfaces have been extensively studied, due to the potential applications of these materials in sensors, organic light-emitting diodes, organic photovoltaic cells, and electrical (charge) storage devices [1–3]. Langmuir–Blodgett (LB) techniques, electropolymerization, and layer-by-layer self-assembly have been used to deposit thin films of PANI on a variety of electrode materials [e.g. 4–6]. In the self-assembly method, adsorption of dissolved PANI from solution is alternated with adsorption of a dissolved polyanion (e.g., sulfonated PANI) [1,5,7–9]. Relative to LB deposition, self-assembly is advantageous due to both its technical simplicity and inherent flexibility; a number of parameters such as substrate surface charge and solution ionic strength can be varied to adjust film structural properties. Due to the physical and chemical heterogeneity of electrode surfaces, it is difficult to prepare homogenous, ultrathin films by electropolymerization; thus self-assembly offers better control over film thickness, uniformity, and surface roughness.

PANI thin films are attractive for sensing applications because their equilibrium redox potential is sensitive to both changes in pH (due to proton doping of the emeraldine base form of PANI) and changes in the redox potential of the surrounding medium [2,10–12]. For example, Lindfors and Ivaska have shown the viability of using PANI as a potentiometric transduction layer on transparent metal oxide substrates [13–16]. Since both the doping/de-doping equilibrium in the oxidized PANI layers and the equilibrium potential of the leucoemeraldine/emeraldine redox couple are pH dependent, PANI films in intimate contact with metal oxide layers can enhance the potentiometric response of the metal oxide film toward changes in

* Corresponding author. Tel.: +1 520 621 9761; fax: +1 520 621 8407.
E-mail address: saavedra@email.arizona.edu (S.S. Saavedra).

0039-9140/$ – see front matter © 2004 Elsevier B.V. All rights reserved.
doi:10.1016/j.talanta.2004.07.053

pH. The use of transparent conducting oxides, such as indium-tin oxide (ITO), also opens up the possibility of simultaneously using optical sensor transduction methods [17,18].

An apparent disadvantage of PANI for sensing applications is that a highly acidic environment (pH < 5) has been thought to be required to generate the protonated, redox-active, conductive form [19]. Recent reports, however, have demonstrated that electrode-supported films composed of PANI and an acidic polyanion (e.g., poly(acrylic acid), PAA) are voltammetrically and potentiometrically active at neutral pH [20,21]. This finding has led to the creation of biocatalytic sensing materials based on PANI/PAA thin films with attached enzymes [22].

Layer-by-layer self-assembly of conducting polymer (CP) films is a relatively recent development; much of the research activity reported to date has focused on the conducting properties of these films in highly acidic solutions [5,8,9]. To our knowledge, characterization of self-assembled CP films at neutral pH has not been reported. Formation of PANI films on ITO allows their properties to be studied using UV–vis spectroelectrochemistry [8,13,14,23]; however, for ultrathin CP films, the sensitivity of measurements in a transmission geometry is generally poor. Enhanced sensitivity can be achieved by performing the measurement in an attenuated total reflection (ATR) geometry at the surface of a planar waveguide. Here we describe the use of visible ATR spectroelectrochemistry, employing an ITO-coated, multimode waveguide to characterize the spectral/redox properties of ultrathin, self-assembled PANI/PAA films at neutral pH. This approach allows redox-associated optical absorbance changes in these films to be measured with an unprecedented level of sensitivity.

2. Experimental

2.1. Materials

The following chemicals were obtained from Aldrich and used without further purification: poly(aniline), emeraldine base, M_n 10000; 1-methyl-2-pyrrolidinone (NMP), anhydrous, 99.5%; poly(acrylic acid), M_n 2000. Poly(aniline) was dissolved in NMP and poly(acrylic acid) was dissolved in deionized (DI) water (18 MΩ cm). Buffer solutions were prepared by dissolving Na_2HPO_4 in DI water at a concentration of 0.1 M and adjusting the pH to 7.0 by adding NaOH or HCl.

Polished soda-lime float glass, 1 mm thick, coated with indium-tin oxide (ITO), was purchased from Applied Films Corporation. The ITO layer thickness was around 84 nm with a refractive index of 1.91 (measured by ellipsometry at 633 nm at a reflection angle of 70°) and the sheet resistance was ≤20 Ω per square. ITO-coated substrates were cut into 1 in. × 3 in. pieces to fit the electrochemical cell. Substrates were cleaned by sequential sonication for 15 min in 2% Triton X-100, DI water, and ethanol, then dried under a nitrogen stream just prior to use.

2.2. PANI/PAA/PANI/PAA thin films

Films composed of alternating layers of PANI and PAA were prepared on clean ITO-coated substrates using the layer-by-layer self-assembly technique [5,8]. The concentrations of the PANI and PAA solutions were 1 and 15 mg/ml, respectively. The deposition time for each layer was 15 min, followed by rinsing with DI water for 15 s, then soaking in DI water for 5 min. After deposition of two bilayers, the ITO/PANI/PAA/PANI/PAA assembly was gently dried under a nitrogen gas stream, then immediately mounted in the spectroelectrochemical cell. Film thickness was measured on dried films using a Sentech Instruments SE 400 ellipsometer. The wavelength was 633 nm, the reflection angle was 70°, and the refractive index of the film was assumed to be 1.46.

2.3. ATR spectroelectrochemistry

A flow cell (Fig. 1) was constructed to perform simultaneous electrochemical and ATR measurements. A 0.5 mm silicone gasket defined a volume of approximately 0.1 ml between a Teflon base and the ITO-coated substrate. The active electrode area was 1 cm^2. Connecting tubing mounted into entrance and exit ports in the Teflon base allowed the solution in the cell to be exchanged. The reference electrode (Ag/AgCl) was inserted in the center of the Teflon base. The counter electrode (a Pt wire) was inserted at the entrance and exit ports. A thin brass sheet was used to make contact with the ITO-coated substrate, which was the transparent working electrode. The potential was controlled using an EG&G potentiostat (Princeton Applied Research, model 263A).

Broadband visible ATR spectroscopy was performed using an instrument built in our lab. A detailed description has been provided in a previous paper [24]. For the experiments reported here, silica prisms (n = 1.46) were used to couple the light beam into and out of the ITO-coated substrate. No polarizer was used so the beam polarization was a mixture of s and p. The internal reflection angle in the soda-lime glass substrate was 64.8°. The distance between the incoupling and outcoupling prisms was 40 mm, which produced 9–10 total internal reflections.

3. Results and discussion

Films composed of two bilayers of PANI and PAA, denoted PANI/PAA/PANI/PAA, were self-assembled on ITO. The ellipsometric thickness of two bilayer films was 2.5 nm. A background subtracted cyclic voltammogram of a PANI/PAA/PANI/PAA film in contact with pH 7.0 buffer is shown in Fig. 2a. Oxidation of the film produced an asymmetric peak, centered at ca. 0.05 V versus Ag/AgCl, but with considerable additional oxidative charge passed out to po-

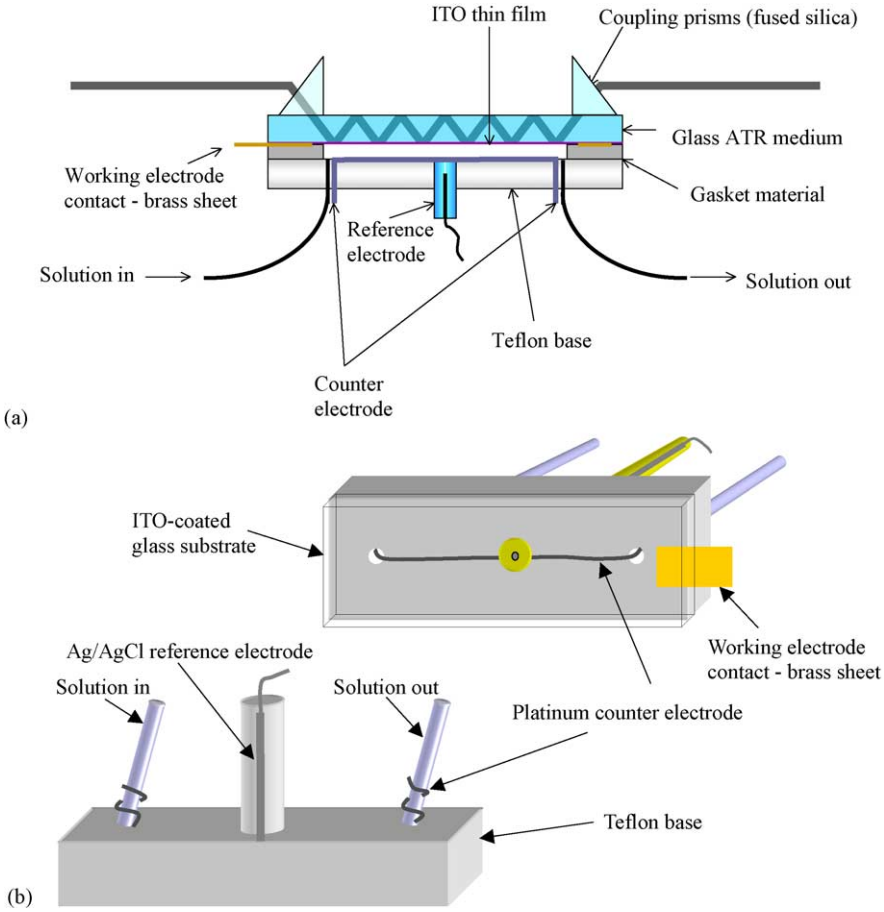

Fig. 1. Experimental arrangement for ATR spectroelectrochemistry (a) and schematic of the flow cell (b). The counter, reference, and working electrodes were Ag/AgCl, platinum, and the ITO-coated substrate, respectively.

tentials of nearly 1.0 V. The reduction of the film back to its initial composition, however, was accomplished in a single, symmetric wave, centered at −0.06 V.

The observation of a single redox process at neutral pH is consistent with the voltammetric behavior reported by Willner and coworkers [22] for PANI films electropolymerized on gold in the presence of PAA. In the absence of PAA, or comparable anionic polymers, PANI is reported to be redox-active only in acidic solutions [19], which precludes its use as a component of biosensors that require neutral pH to maintain bioactivity [22]. Furthermore, two distinct redox reactions are generally observed for PANI films at low pH [20].

The voltammetry of PANI/PAA/PANI/PAA films was also found to vary with pH. Two redox processes were observed at pH ≤ 3 (data not shown): (i) the first with a formal reduction potential of ca. 0.16 V, corresponding to oxidation of the fully reduced leucoemeraldine to the partially oxidized emeraldine, and (ii) a second with a formal reduction potential of ca. 0.31 V, corresponding to oxidation of the partially oxidized emeraldine to the fully oxidized pernigraniline [20,25]. As the pH was increased above 5, these two redox processes merged into a single oxidation/reduction process, albeit with a loss of some electrochemical activity. This behavior is consistent with published studies of pH effects on the cyclic voltammetric behavior of PANI films electropolymerized on glassy carbon electrodes in the presence of PAA [20].

The full-width at half-maximum (fwhm) of the anodic peak in Fig. 2a was 170 mV whereas the fwhm of the cathodic peak was 103 mV. Integration of the charge under the cathodic and anodic peaks yielded equivalent values (ca. 5×10^{-5} C/cm^2). We conjecture that the broader anodic peak is attributable to changes in film structure accompanying the redox reaction, corresponding to the slow incorporation of counter ions during polymer oxidation. Oxidation of the neutral polymer generates electrostatic repulsion between the positively charged polymer chains, resulting in changes in chain conformation, counter ion migration to maintain neutrality, and solvent migration to occupy voids in the expanded film. Thus the oxidation process is likely to be limited by the rate of conformational change and the rate of counter ion and solvent transport [26–29].

In contrast, during the reduction process, the polymer chains are neutralized; counter ions and solvent molecules may readily migrate out of the relaxed structure of the polymer chains (or additional, small cations may migrate in), pro-

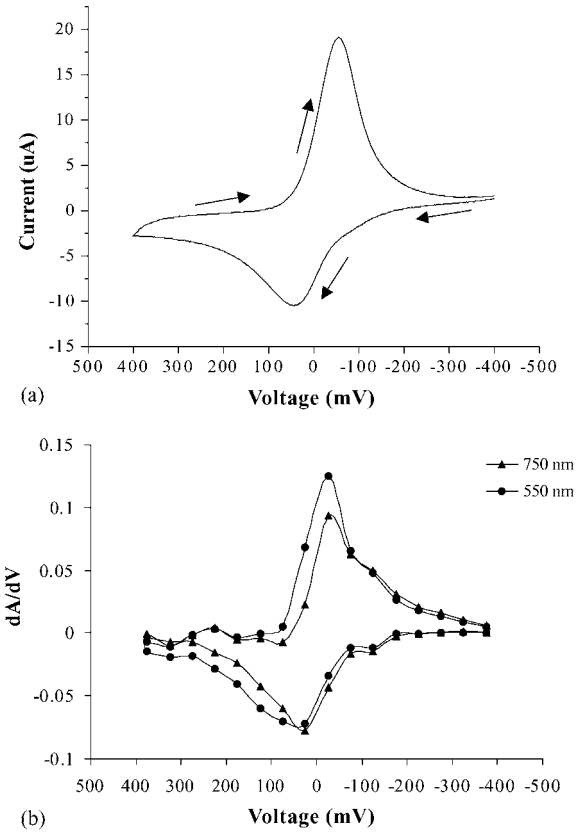

Fig. 2. (a) Cyclic voltammogram of a self-assembled PANI/PAA/PANI/PAA film in contact with 0.1 M phosphate buffer (pH 7.0). The scan was initiated at −400 mV at a rate of 50 mV/s. (b) Absorpto-voltammograms of a PANI/PAA/PANI/PAA self-assembled film in contact with 0.1 M, pH 7 phosphate buffer. The potential was scanned at 5 mV/s and spectra were acquired at a rate of one per 10 s. The derivative of the absorbance at both 550 nm (circles) and 750 nm (triangles) as a function of potential is plotted at 50 mV intervals. The *x*-axis values denote the center of the 50 mV range in which the respective spectrum was acquired (e.g., the spectrum acquired during scanning from 300 to 350 mV was assigned an *x*-axis value of 325 mV).

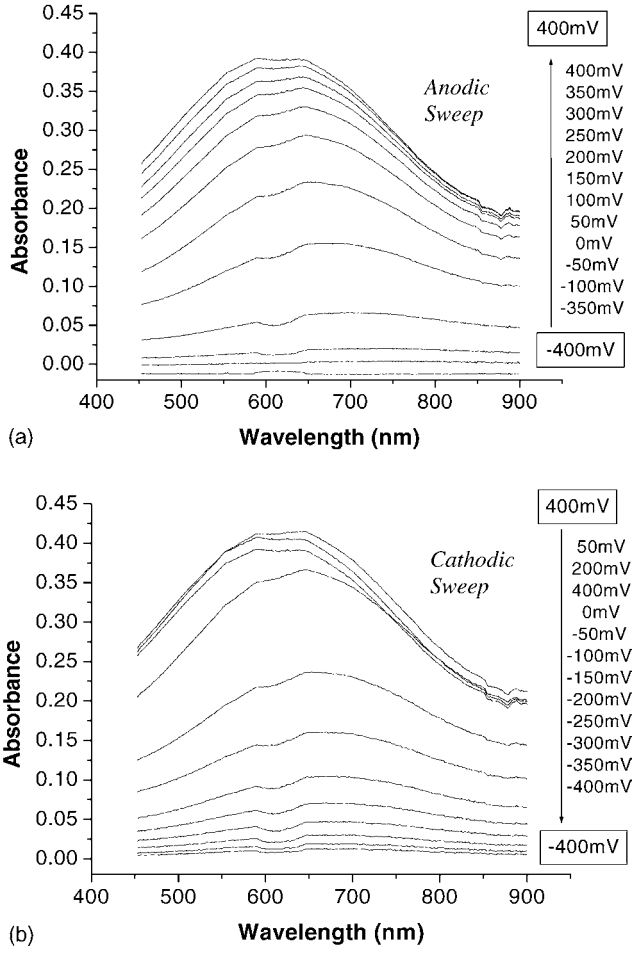

Fig. 3. ATR spectra of a self-assembled PANI/PAA/PANI/PAA film in contact with 0.1 M, pH 7.0 phosphate buffer, acquired during oxidation (a) and reduction (b) at 50 mV intervals between −400 and 400 mV. The scan rate was 5 mV/s. Due to the similarity and overlap of spectra near the positive and negative limits of the potential range, not all spectra are shown.

ducing a more compact polymer film structure. Therefore, the reduction process in oxidatively doped conducting polymer films should be less affected by the rates of restructuring of the polymer film and transport of counter ions and solvent [26–29].

The electroactivity of PANI in these films can be estimated from the voltammetric and ellipsometric data. The volume occupied by one aniline repeat unit is estimated to be 42.5 Å^3. The total thickness of the two PANI layers in a PANI/PAA/PANI/PAA film is approximately 1 nm, which yields a total PANI surface coverage of $\sim 4 \times 10^{-9}$ mol of repeat units per cm^2. By integrating the reductive current measured from an ITO electrode area of 1 cm^2, the surface coverage of electroactive PANI was calculated to be 5×10^{-10} mol of repeat units per cm^2. Therefore, only ca. 12.5% of PANI in the PANI/PAA/PANI/PAA film is electroactive at pH 7. Since the fraction of electroactive PANI is higher at lower pH [30], these results suggest that the self-assembly protocol employed here yields a restricted microstructure for the poly(aniline) chains at neutral pH, i.e. there are regions of PANI which are folded compactly, and thus are unable to accommodate the incorporation of counter ions that accompany oxidative doping of the polymer. Work in progress suggests that the fraction of electroactive PANI at higher pH can be enhanced with optimization of the self-assembly process.

Waveguide spectroelectrochemistry of PANI/PAA/PANI/PAA films was performed at a scan rate of 5 mV/s, which allowed broadband ATR spectra to be acquired at 50 mV intervals during both oxidation and reduction. Spectra were ratioed to the spectrum at −400 mV, which was taken as the blank. Typical spectra are plotted in Fig. 3. It is readily apparent that the multiple-reflection ATR geometry provides adequate sensitivity to probe PANI/PAA/PANI/PAA films on ITO, although these films are in most cases considerably thinner than PANI films studied by other groups using transmission spectroelectrochemical methods [8,13,14,23]. Excellent sensitivity was obtained because, based on a comparison of spectra measured at open circuit potential (data not shown), the evanescent thin film pathlength in the ATR geometry is

about 35 times greater than the optical pathlength of a conventional, single pass transmission geometry. Thus even spectra of lightly oxidized PANI/PAA/PANI/PAA films (which were very weakly absorbing; see below and Fig. 3) were measured with good sensitivity.

The visible absorbance of PANI arises from the partially oxidized emeraldine, which is blue (λ_{max} = 620 nm), and the fully oxidized pernigraniline form, which is purple (λ_{max} = 580 nm) [31,32]. The anodic sweep, corresponding to the spectra in Fig. 3a, was initiated at −400 mV, where the predominant form of PANI is the fully reduced, optically transparent leucoemeraldine. At pH 7 in these PANI/PAA/PANI/PAA films, oxidation of leucoemeraldine to the emeraldine and pernigraniline forms proceeds simultaneously (consistent with the single redox process observed in Fig. 2a). Thus at potentials more positive than 0 V, PANI is converted into a mixture of emeraldine and pernigraniline, as indicated by an increase in absorbance across the entire spectral range of 450–900 nm (Fig. 3b). However, the change in absorbance as a function of potential was not constant across this wavelength interval. Between 0 V and 300 mV, the absorbance increase was greater at longer wavelengths (>620 nm) relative to that at shorter wavelengths (<620 nm). Between 300 and 400 mV, the opposite trend was observed. This behavior is consistent with the known differences in λ_{max} and oxidation state of the emeraldine and pernigraniline forms [31,32]. At intermediate potentials (0–300 mV), emeraldine is the predominate form, which corresponds to an observed λ_{max} > 620 nm. At more positive potentials (>300 mV), pernigraniline is the major form, which produces a blue shift in the observed λ_{max}. The “saddle” in the spectra centered around 620 nm is attributed to partial resolution of the emeraldine and pernigraniline absorbance bands.

ATR spectra acquired during the cathodic sweep, initiated at 400 mV, are plotted in Fig. 3b. The spectral transitions were similar to those observed during oxidation. At potentials >0 mV, the extent of pernigraniline reduction was greater than that of emeraldine, which produced a red shift in the spectrum, characteristic of the emeraldine form. At potentials <0 mV, conversion to the leucoemeraldine form was observed, accompanied by a gradual decline in absorbance intensity.

From a comparison of Fig. 3a and b, however, it is clear that the rate of spectral change as a function of potential was different during the anodic and cathodic scans. Minimal changes in the absorbance spectrum were observed during the cathodic sweep until the potential reached 0 mV. Between 0 and −50 mV, about 33% of the total decline in absorbance was observed (Fig. 3b). In contrast, the absorbance increase during the anodic scan (Fig. 3a) was relatively constant as a function of potential. This difference is consistent with the voltammetric data plotted in Fig. 2. As discussed above, the rate of oxidation of PANI/PAA/PANI/PAA films appears to be limited by changes in chain conformation, counter ion migration to maintain neutrality, and solvent migration to occupy voids in the expanded film [26–29]. Thus the rate of spectral change as a function of potential should be more gradual during oxidation than during reduction, as is observed in Fig. 3.

Lastly, the absorpto-voltammograms plotted in Fig. 2b were reconstructed from the spectroelectrochemical data at both 550 nm (where the absorbance of the pernigraniline form is greater) and 750 nm (where the absorbance of the emeraldine form is greater). The overall shapes of both curves match the cyclic voltammogram in Fig. 2a quite well (although background subtraction was not required, since the ATR method is insensitive to non-Faradaic processes). However, at 750 nm the onset of the oxidation process occurred at slightly less positive voltages relative to 550 nm, which is consistent with the differences in λ_{max} and oxidation state of the emeraldine and pernigraniline forms noted above [31,32]. During the initial part of the oxidative sweep, conversion to emeraldine predominates; thus the absorbance increase is more pronounced at >620 nm relative to shorter wavelengths. At more positive voltages, conversion to pernigraniline predominates, which produces the increased absorbance at shorter wavelengths. This comparison clearly demonstrates that the electrochemical reactions of ultrathin PANI films can be spectroscopically monitored in real time.

In conclusion, redox-associated optical absorbance changes in self-assembled, conducting, ultrathin PANI/PAA/PANI/PAA films were monitored at neutral pH using a multiple reflection, broadband ATR spectrometer. The sensitivity of this arrangement is approximately 35 times greater than that of a conventional, single pass transmission geometry, making it feasible to perform measurements on lightly oxidized, weakly absorbing films. Furthermore, the combination of cyclic voltammetry and broadband ATR spectroscopy at the surface of an ITO-coated, planar waveguide electrode allows the redox behavior of ultrathin PANI films to be examined in real time (i.e., during potential scanning). More detailed ATR and electrochemical studies of these ultrathin PANI/PAA/PANI/PAA films as pH sensors are in progress, including a comparison of their potentiometric and optical responses.

Acknowledgment

This work was supported by Grant No. DE-FG02-02ER15378 from Chemical Sciences, Geosciences and Biosciences Division, Office of Basic Energy Research, U.S. Department of Energy.

References

[1] K. Peter, H. Ho, M. Granström, R.H. Friend, N.C. Greenham, Adv. Mater. 10 (1998) 769.
[2] A.A. Karyakin, M. Vuki, L.V. Lukachova, E.E. Karyakina, A.V. Orlov, G.P. Karpachova, J. Wang, Anal. Chem. 71 (1999) 2534.

[3] W. Chun-Guey, H. Hsia-Tsai, Y. Yuh-Ruey, J. Mater. Chem. 11 (2001) 2287.
[4] A. Dhanabalan, R.B. Dabke, S.N. Datta, N.P. Kumar, S.S. Major, S.S. Talwar, A.Q. Contractor, Thin Solid Films 295 (1997) 255.
[5] J.H. Cheung, W.B. Stockton, M.F. Rubner, Macromolecules 30 (1997) 2712.
[6] H. Okamoto, M. Okamoto, T. Kotaka, Polymer 39 (1998) 4359.
[7] A. Baba, M. Park, R.C. Advincula, W. Knoll, Langmuir 18 (2002) 4648.
[8] D. Li, Y. Jiang, C. Li, Z. Wu, X. Chen, Y. Li, Polymer 40 (1999) 7065.
[9] J. Paloheimo, K. Laakso, H. Isotalo, H. Stubb, Synth. Met. 68 (1995) 249–257.
[10] D.W. Hatchett, M. Josowicz, J. Janata, J. Phys. Chem. B 103 (1999) 10992.
[11] H. Sangodkar, S. Sukeerthi, R.S. Srinivasa, R. Lal, A.Q. Contractor, Anal. Chem. 68 (1996) 779.
[12] H.S. Moon, J.K. Park, Macromolecules 31 (1998) 6461.
[13] T. Lindfors, A. Ivaska, J. Electroanal. Chem. 531 (2002) 43.
[14] T. Lindfors, A. Ivaska, J. Electroanal. Chem. 535 (2002) 65.
[15] T. Lindfors, A. Ivaska, Anal. Chim. Acta 437 (2001) 171.
[16] T. Lindfors, A. Ivaska, Anal. Chim. Acta 404 (2000) 111.
[17] E.S. Matveeva, C.F. Gimenez, M.J.G. Tejera, Synth. Met. 123 (2001) 1175.
[18] E.C. Venancio, C.A.R. Costa, S.A.S. Machado, A.J. Motheo, Electrochem. Commun. 3 (2001) 229.
[19] (a) T. Ohsaka, Y. Ohnuki, N. Oyama, K. Katagiri, J. Kamisako, J. Electroanal. Chem. 161 (1984) 399;
(b) S.Y. Cui, S.M. Park, Synth. Met. 105 (1999) 91.
[20] P.N. Bartlett, E. Simon, Phys. Chem. Chem. Phys. 2 (2000) 2599.
[21] P.N. Bartlett, E.N.K. Wallace, Phys. Chem. Chem. Phys. 3 (2001) 1491.
[22] O.A. Raitman, E. Katz, A.F. Bückmann, I. Willner, J. Am. Chem. Soc. 124 (2002) 6487.
[23] A. Malinauskas, R. Holze, Synth. Met. 97 (1998) 31.
[24] W.J. Doherty III, C.L. Donley, N.R. Armstrong, S.S. Saavedra, Appl. Spectrosc. 56 (2002) 920.
[25] W.S. Huang, B.D. Humphrey, A.G. MacDiarmid, J. Chem. Soc., Faraday Trans. 82 (1986) 2385.
[26] (a) S.W. Feldberg, A.R. Bruckenstein, J. Am. Chem. Soc. 106 (1984) 4671;
(b) I. Feldberg, Rubenstein, J. Electroanal. Chem. 240 (1988) 1.
[27] (a) A.R. Hillman, M.J. Swann, S. Bruckenstein, J. Phys. Chem. 95 (1991) 3271;
(b) S. Bruckenstein, A.R. Hillman, J. Phys. Chem. 95 (1991) 10748.
[28] T.F. Otero, H. Grande, J. Rodriguez, Synth. Met. 83 (1996) 205.
[29] T.F. Otero, in: R.E. White, O'M. Bockris, B.E. Conway (Eds.), Modern Aspects of Electrochemistry, vol. 33, Kluwer Academic/Plenum Publishers, New York, 1999, p. 307.
[30] C. Ge, N.R. Armstrong, S.S. Saavedra, unpublished results.
[31] P.M. McManus, R.J. Cushman, S.C. Yang, J. Phys. Chem. 91 (1987) 744.
[32] M.K. Ram, G. Mascetti, S. Paddeu, E. Maccioni, C. Nicolini, Synth. Met. 89 (1997) 63.